Glia (2015.4) 63(4):595-610.

Interferon regulatory factor 7 participates in the M1-like microglial polarization switch

Tatsuhide Tanaka, Koichi Murakami, Yoshio Bando, Shigetaka Yoshida

Interferon regulatory factor 7 participates in the M1-like microglial polarization switch

Tatsuhide Tanaka†, Koichi Murakami, Yoshio Bando and Shigetaka Yoshida

Department of Functional Anatomy and Neuroscience, Asahikawa Medical University, Midorigaoka-higashi 2-1-1-1 Asahikawa, Hokkaido 078-8510, Japan

†Corresponding author:

Tatsuhide Tanaka

Tel.: +81-166-68-2303; Fax: +81-166-68-2309; E-mail: ttanaka@asahikawa-med.ac.jp

Running title: Polarization switch in microglia

Number of figures: 6

Number of supplementary figures: 7

Number of tables: 0

Number of pages: 38

Abstract: 196 words

Introduction: 553 words

Materials and Methods: 1,250 words

Results: 2,255 words

Discussion: 1,633 words

References: 1,600 words

Figure legends: 1,284 words

Total: 8,968 words

Main points:

Microglial phenotypes are regulated by extracellular stimulus.

Interferon regulatory factor 7 is elevated in M1-like microglia and is associated with microglial polarization.

KEY WORDS: microglia, M1, M2, polarization, IRF7

ABSTRACT

Microglia are generally considered the immune cells of the central nervous system. Recent studies have demonstrated that under specific polarization conditions, microglia develop into two different phenotypes, termed M1-like and M2-like microglia. However, the phenotypic characteristics of M1-like- and M2-like-polarized microglia and the mechanisms that regulate polarization are largely unknown. In this study, we characterized LPS-treated M1-like and IL-4-treated M2-like microglia and investigated the mechanisms that regulate phenotypic switching. The addition of M2-like microglial conditioned medium (CM) to primary neurons resulted in an increase in neurite length compared with neurons treated with M1-like microglial CM, possibly because of the enhanced secretion of neurotrophic factors by M2-like microglia. M1-like microglia were morphologically characterized by larger soma, while M2-like microglia were characterized by long processes. M2-like microglia exhibited greater phagocytic capacity than M1-like microglia. These features switched in response to polarization cues. We found that expression of interferon regulatory factor 7 (IRF7) increased during the M2-like to M1-like switch in microglia *in vitro* and *in vivo*. Knockdown of IRF7 using siRNA suppressed the expression of M1 marker mRNA and reduced phosphorylation of STAT1. Our findings suggest that IRF7 signaling may play an important role in microglial polarization switching.

INTRODUCTION

Microglia, widely considered the immune cells of the central nervous system (CNS), are involved in many types of inflammatory processes in the brain (Hanisch and Kettenmann, 2007; David and Kroner, 2011). They are critical in developmental processes and are essential for the maintenance of neuronal homeostasis (Ueno et al., 2013; Saijo and Glass, 2011). Microglia have been proposed to be involved in the pathogenesis of neurodegenerative diseases (Perry et al., 2010; Biber et al., 2014). However, microglia have also been shown to support cell survival during tissue repair following CNS injury (David and Kroner, 2011; Olah et al., 2012). Previously, we provided evidence for a role of microglia in axonal regeneration and remyelination (Tanaka et al., 2009, Tanaka et al., 2013). Because of these contrasting properties of microglia, there has been considerable debate as to whether the microglial response is beneficial or detrimental for tissue protection and repair (David and Kroner, 2011). Recent studies have demonstrated that under specific polarization conditions, microglia can develop into either of two distinct phenotypes (David and Kroner, 2011; Ajmone-Cat et al., 2013). However, the mechanisms regulating microglial plasticity and polarization are largely unknown.

Macrophages can be polarized into two phenotypes (Sica and Bronte. 2007; Liu et al., 2014). Classically activated macrophages (M1 macrophages) are pro-inflammatory and have a central role in host defense against infection, while alternatively activated macrophages (M2 macrophages) are associated with responses to anti-inflammatory reactions and tissue remodeling (Liu et al., 2014). Monocytes that circulate in the bloodstream are recruited to inflamed tissues and give rise to macrophages. However, it has been reported that M2 macrophages accumulate independently of monocytes and are derived from tissue macrophages through self-renewal (Jenkins et al., 2011). It has also been reported that endogenous mediators, such as transcription factors, regulate macrophage activation (Durafourt et al., 2012; Sica and Mantovani. 2012; Liu et al., 2014). Recent studies show that

microglia are derived from primitive myeloid progenitors in the yolk sac, and that the origin of microglia differ from monocytes and tissue macrophages (Ginhoux et al., 2010). Furthermore, many studies have shown that microglia and macrophages differ in their responsiveness to stimuli (Schmid et al., 2009, Melief et al., 2012; Beutner et al., 2013; Butovsky et al., 2014).

Although the mechanisms underlying macrophage polarization have been intensively studied, little is known about the polarization of microglia. As mentioned above, microglia are distinct from macrophages and their gene expression. Therefore, we refer to M1-like microglia as detrimental microglia and M2-like microglia as protective microglia in this paper. M1-like microglia release destructive proinflammatory mediators and cause damage to healthy tissue (Perry et al., 2010; Chhor et al., 2013). Conversely, M2-like microglia possess protective properties and promote tissue remodeling and repair (Perry et al., 2010; Miron et al., 2013). It is not clear if M1-like and M2-like microglia are derived from resting-state microglia, or whether they are derived from a phenotypic shift from one form to the other. We hypothesized that microglia respond dynamically to their surroundings, switching phenotypically from M1-like to M2-like or M2-like to M1-like microglia. In this study, we investigate M1-like and M2-like microglial gene expression, morphology, and phagocytic activity, and we examine whether polarization switching occurs in response to extracellular stimuli. Furthermore, we explore the role of interferon regulatory factor 7 (IRF7), an endogenous transcription factor, in regulating microglial activation.

MATERIALS AND METHODS

The experimental procedures using animals were approved by the Institutional Animal Care and Use Committee of Asahikawa Medical University.

Cell Culture

Primary cultures of microglial cells were obtained from C57BL/6 mice on postnatal day 1 (P1). Briefly, the mouse cerebral cortex was digested with 0.25% trypsin and DNase for 15 min. Cells were passed through a 70-μm nylon mesh. The resultant cell suspension was diluted with DMEM supplemented with 10% FBS and 1% penicillin/streptomycin and seeded into a culture flask. Microglial cells within the astrocyte monolayer sheet were removed by shaking.

Reagents for Cell Culture

Reagents used in this study were as follows: lipopolysaccharide (LPS, 1 μg/mL; Sigma, St. Louis, MO, USA) and recombinant mouse IL-4 (20 ng/mL; R&D systems, Minneapolis, MN, USA). IRF7 siRNA (20 nM) (stealth siRNA; Invitrogen, Stockholm, Sweden) or control siRNA (20 nM) (Stealth RNAi negative control; Invitrogen) were transfected into microglia with Lipofectamine 2000 (Invitrogen) according to manufacturer's protocol. After 30 h of transfection, the cells were treated with LPS or IL-4. siRNA were of the following sequences: IRF7 #1 sense, 5′-CCAGUCCUGCUGAGCUCCCAGAUCA-3′; IRF7 #1 antisense, 5′-UGAUCUGGGAGCUCAGCAGGACUGG-3′; IRF7 #2 sense, 5′-CGAGUGCUGUUUGGAGACUGGCUAU-3′; IRF7 #2 antisense, 5′-AUAGCCAGUCUCCAAACAGCACUCG-3′; IRF7 #3 sense, 5′-GGGAUCCAGUUGAUCCGCAUAAGGU-3′; IRF7 #3 antisense, 5′-ACCUUAUGCGGAUCAACUGGAUCCC-3′.

Preparation of Microglial Conditioned Media

Microglial cells were plated in 3.5-cm dishes and incubated with LPS or IL-4. After an 18-h incubation, conditioned medium (CM) from these activated microglia was transferred to wells containing 1×10^5 cortical neurons at 1 day *in vitro*. Neurite outgrowth assay and qRT-PCR were performed 48 h after treatment with the CM.

Phagocytosis Assay

Microglia were plated in 24-well plates and incubated with LPS or IL-4. Fluorescently labeled latex beads (1.0 μm; PolyScience, Warrington, PA, USA) were opsonized with 50% FBS for 30 min at 37 °C before the experiments. Microglia were incubated with the opsonized latex beads (2×10^6 particles/well) for 1 h at 37 °C. Subsequently, microglia were washed with PBS and fixed with 4 % paraformaldehyde for 1 h. Microglia were stained with an anti-Iba1 (1:500; Wako, Osaka, Japan) antibody, and the uptake of the fluorescent latex beads was assessed under a fluorescence microscope.

Morphological Analysis of Cultured Microglia

The cell perimeter (μm) and cell area (μm^2) were determined over seven separate experiments, and the transformation index (TI), reflecting the degree of process extension, was calculated using the equation [perimeter of cell (μm)]^2/4π [cell area (μm^2)], as previously described (Fujita et al., 1996).

Contusive Spinal Cord Injury (SCI)

Female 8- to 10-week-old Balb/c mice were obtained from the Animal Laboratory for Medical Research of Asahikawa Medical University. Mice were anesthetized with an intraperitoneal (IP) injection of sodium pentobarbital (40–50 mg/kg body weight). The mice were placed in a prone position, and a midline incision was made in the skin. Under a

dissecting microscope, a laminectomy at the 8th thoracic (T8) level was performed, and the dura mater was exposed. A 3-g weight was dropped from a height of 5 cm onto the exposed spinal cord (Murakami et al., 2013).

Experimental Induction of Demyelination

Demyelination was induced by feeding a diet containing 0.2% cuprizone (bis-cyclohexanone oxaldihydrazone; Sigma) mixed into a ground standard rodent chow. For remyelination, animals were returned to the normal diet after cuprizone treatment. Age-matched control mice were maintained on the same diet without cuprizone.

Tissue Preparation

Mice were anesthetized with sodium pentobarbital (100 mg/kg, IP) and perfused transcardially with saline, followed by 4% paraformaldehyde (PFA) in 0.1 M phosphate buffer (PB, pH 7.4). Brains or spinal cords were removed, postfixed overnight in the same fixative, and then immersed in 30% sucrose in 0.1 M PB overnight. Brains or spinal cords were then frozen in powdered dry ice, embedded in Tissue-Tek OCT compound (Sakura Finetek, Torrance, CA, USA), and stored at −80 °C prior to sectioning. Frozen 20-μm transverse sections of the brain were cut on a cryostat and mounted onto glass slides.

Immunohistochemistry

The sections were immersed in 0.1 M PB containing 5% bovine serum albumin (BSA) and 0.3% Triton X-100 for 1 h. Anti-Iba1 (1:500; Wako), anti-CD86 (1:200; abcam, Cambridge, MA, USA), anti-ED1 (CD68) (1:100; AbD Serotec, Raleigh, NC, USA) or anti-IRF7 (1:50; Santa Cruz Biotechnology, Inc., Santa Cruz, CA, USA) antibody was applied overnight at 4 °C. Alexa Fluor 488-conjugated anti-mouse IgG (1:1000; Life Technologies, Grand Island, NY, USA), Alexa Fluor 568-conjugated anti-rabbit IgG (1:1000, Life Technologies) were

used as the secondary antibody. The images were obtained on a confocal laser scanning microscope with Fluoview FV1000-D software (Olympus, Tokyo, Japan).

Immunocytochemistry

Cultured cells were fixed with 4% PFA in 0.1 M PB for 1 h at room temperature and incubated with blocking solution containing 5 % BSA and 0.3 % Triton X-100 in PBS for 1 h. Primary antibodies, anti-CD86 (1:1000; Abcam), anti-Arg-1 (1:100; Santa Cruz), anti-β-tubulin III (Tuj1) (1:1 000; Covance, Princeton, NJ, USA), anti-Iba1 (1:500; Wako), anti-ED1 (1:100; AbD Serotec) or anti-IRF7 (1:50; Santa Cruz) were applied overnight at 4 °C. Alexa Fluor 488-conjugated anti-mouse IgG (1:1000; Life Technologies) or Alexa Fluor 568-conjugated anti-rabbit IgG (1:1 000, Life Technologies) were used as the secondary antibody.

qRT-PCR

Total RNA was extracted using TRIzol (Life Technologies) and converted to cDNA with reverse transcriptase using oligo$(dT)_{20}$ primers to prime AMV reverse transcriptase (Promega, Madison, WI, USA) according to the manufacturer's instructions. Specific DNAs were mixed and amplified with 0.5 μM of each PCR primer and cDNA. The following primers were used in this study: Arg1 sense primer, 5′-GCGCCTTTCTCAAAAGGACAGC-3′; Arg1 anti-sense primer, 5′-TGGCTTTCCCCACAGACCGTG-3′; BDNF sense primer, 5′-GCGGCAGATAAAAAGACTGC-3′; BDNF anti-sense primer, 5′-CTTATGAATCGCCAGCCAAT-3′; CCL5 sense primer, 5'-GCCTCACCATATGGCTCGGACACCA-3'; CCL5 anti-sense primer, 5'-TGGGTTGGCACACACTTGGCGGTT-3', CD206 sense primer, 5′-TCTGTTCAGCTATTGGACGCGA-3′; CD206 anti-sense primer, 5′-TTTGATGGCACTCCCAAACA-3′; CD86 sense primer,

5′-CCCAGATGCACCATGGGCTTGGCAA-3′; CD86 anti-sense primer,

5′-AAGCTCGTGCGGCCCAGGTACT-3′; CXCL1 sense primer,

5’-GCCTATCGCCAATGAGCTGCGCT-3’; CXCL1 anti-sense primer,

5’-AAGGCAAGCCTCGCGACCATTC-3’, GAPDH sense primer,

5′-CTACATGGTCTACCTGTTCCAG-3′; GAPDH anti-sense primer,

5′-AGTTGTCATGGATGACCTTGG-3′; IGF-1 sense primer,

5′-ACAGCTGGACCAGAGACCCTTTGC-3′; IGF-1 anti-sense primer,

5′-GGCTTCAGTGGGGCACAGTA-3′; IL-1β sense primer,

5′-CTCCATGAGCTTTGTACAAGG-3′; IL-1β anti-sense primer,

5′-TGCTGATGTACCAGTTGGGG-3′; IL-1RI sense primer,

5′-GCAAGACCCCCATATCAGCGGACC-3′; IL-1RI anti-sense primer,

5′-ATCCCCGGCAATGTGGAGCCGCT-3′; IL-6 sense primer,

5’-ACACATGTTCTCTGGGAAATCG-3’; IL-6 anti-sense primer,

5’-TGAAGGACTCTGGCTTTGTC-3’, iNOS sense primer,

5′-TTGGTGTTTGGGTGCCGGC-3′; iNOS anti-sense primer,

5′-CCATAGGAAAAGACTGCACCGAAG-3′; IRF1 sense primer,

5′-ACCAAATCCCAGGGCTGATC-3′; IRF1 anti-sense primer,

5′-TACACCCGCACAGCAGAGCT-3′; IRF2 sense primer,

5′-ATGCATGCGGCTCGGCACGGAT-3′; IRF2 anti-sense primer,

5′-ATCCGGTAGACTCTGAAGGCGTTGT-3′; IRF3 sense primer,

5′-GGCTGGTGTCACAGCTGGACCTG-3′; IRF3 anti-sense primer,

5′-TGTCAGCAGCTAACCGCAACAC-3′; IRF4 sense primer,

5′-CTGCGGCAATGGGAAACTCC-3′; IRF4 anti-sense primer,

5′-GCTCTTGTTCAGAGCACATCGT-3′; IRF7 sense primer,

5′-GCTATTGGGGGAGGTCAGCA-3′; IRF7 anti-sense primer,

5′-AACGCCCTGTGCTGTGGAG-3′; IRF8 sense primer,

5′-AGCAGCATGTACCCGGGGCTGATCT-3′; IRF8 anti-sense primer, 5′-GGGCTCTTGTTCAGAGCACAGCGT-3′; IRF9 sense primer, 5′-AAGCCTGGGACCTTTTCAGCGGCT-3′; IRF9 anti-sense primer, 5′-TCGGAAGTCTTGCTTGCCTGCAT-3′; MOB3C sense primer, 5’-AGCGCTTCGAGCCTGGCACACA-3’; MOB3C anti-sense primer, 5’-TGACGCTCGTCCTGCCAGCGGTA-3’, NGF sense primer, 5′-TTGATCGGCGTACAGGCAGAACCGT-3′; NGF anti-sense primer, 5′-CTGGGTGCTGAACAGCACACGGGGT-3′; PPARγ sense primer, 5’-CGGAATCAGCTCTGTGGACC-3’; PPARγ anti-sense primer, 5’-AAGGTGGAGATGCAGGTTCT-3’, TNF-α sense primer, 5′-AATTCACTGGAGCCTCGAATG-3′; TNF-α anti-sense primer, 5′-CCCGGCCTTCCAAATAAAT-3′; TNFRII sense primer, 5′-ACACAGTGCCCGCCCAGGTTGT-3′; TNFRII anti-sense primer, 5′-CGCAAGCACACACTCGGTTCTGCT-3′; Ym1 sense primer, 5’-TACCAGTTGGGCTAAGGACA-3’; Ym1 anti-sense primer, 5’-ATCTGACGGTTCTGAGGAGT-3’. qRT-PCR was performed following the protocol in the Light Cycler SYBR Green kit (Roche, Mannheim, Germany).

Western Blotting

Samples were prepared as described previously (Tanaka et al., 2009). Protein concentration was measured using a bicinchoninic acid protein assay kit (Thermo Scientific, Waltham, MA, USA). Equal amounts of protein were subjected to SDS-PAGE and then transferred to a polyvinylidene difluoride membrane (Merck Millipore, Billerica, MA, USA). The blots were probed with anti-phospho-STAT1 (1:1 000; Cell Signaling Technology, Danvers, MA, USA), anti-STAT1 (1:200; Santa Cruz), anti-IRF7 (1:1000; LifeSpan BioSciences, Seattle, WA, USA) or GAPDH (1:5000; Life technologies) antibodies. Blots were then incubated with

horseradish peroxidase-conjugated anti-mouse and anti-rabbit IgG and visualized using ECL western blotting detection reagents (GE Healthcare, Piscataway, NJ, USA). Data were acquired in arbitrary densitometric units using Scion image software.

Statistical Analyses

Statistical analyses were performed using the paired Student's *t*-test or one-way ANOVA, and differences between treatment means were determined with the Tukey-Kramer test.

RESULTS

Polarization of Microglia into M1-like and M2-like Phenotypes

In this study, LPS and IL-4 were used as a proinflammatory and anti-inflammatory stimuli, respectively. We exposed primary microglia to LPS or IL-4 for 18 h and measured expression of mRNAs for CD86, IL-1β, chemokine (C-C motif) ligand 5 (CCL5), IL-6, inducible nitric oxide synthase (iNOS), chemokine (C-X-C motif) ligand 1 (CXCL1), arginase 1 (Arg1), CD206 (also known as Mrc1), IGF-1 and PPARγ. LPS increased mRNA levels of CD86, IL-1β, CCL5, IL-6, iNOS and CXCL1, which are markers of the M1 phenotype (Mantovani et al., 2004; Chhor et al., 2013) (Fig. 1A and Supplemental Fig. 1A). In contrast, IL-4 increased mRNA levels of Arg1, CD206, IGF-1 and PPARγ, markers of the M2 phenotype (Bouhlel et al., 2007; Chhor et al., 2013; Liu et al., 2014) (Fig. 1A and Supplemental Fig. 1A). LPS did not increase expression of M2 markers, and IL-4 did not increase expression of M1 markers (Fig. 1A and Supplemental Fig. 1A). Immunocytochemistry revealed that CD86 was expressed in LPS-treated microglia and that Arg1 was expressed in IL-4-treated microglia (Supplemental Fig. 1B). Our findings demonstrate that LPS induces the M1-like phenotype and that IL-4 induces the M2-like phenotype in microglia.

Characterization of M1 and M2 Microglial Phenotypes

We examined the morphology of M1 and M2 microglia *in vitro* (Fig. 1 and Supplemental Figs. 2 and 3). Most unstimulated microglia had small somata (Fig. 1B and Supplemental Figs. 2 and 3). LPS-treated microglia were characterized by large somata, while IL-4-treated microglia were characterized by long processes (Fig. 1B and Supplemental Fig. 2 and 3). We performed quantitative analysis using the transformation index (TI) value, an indicator of the degree of morphological differentiation (Fujita et al., 1996). If a cell is circular, the TI value is 1, while a cell with long processes has a large value. As shown in Fig. 1C, the TI value was increased in IL-4-treated M2-like microglia (6.10 ± 0.94) compared with unstimulated or

LPS-treated microglia (control, 2.49 ± 0.22; LPS, 3.08 ± 0.32) (Fig. 1C). Most cells tended to polarize towards a specific morphology in response to LPS or IL-4 (Supplemental Fig. 3). We next examined the phagocytic activity of M1-like and M2-like microglia. M1-like microglia exhibited less phagocytic activity than M2-like microglia (Supplemental Fig. 4 and Fig. 2H). Our results differ somewhat from those of Wang and colleagues (Wang et al., 2013). Although they reported that M1-like microglia exhibit less phagocytic activity than unstimulated microglia, M1-like microglia had similar phagocytic activity to control in our model (Supplemental Fig. 4 and Fig. 2H).

To further characterize the M1-like and M2-like phenotypes, M1-like or M2-like microglial CM was added to cultured cortical neurons (Fig. 1D). The addition of M2-like microglial CM resulted in an increase in the length of axons (102.0 ± 4.29 μm) compared with untreated neurons (57.0 ± 5.05 μm), neurons treated with M1-like microglial CM (64.0 ± 2.87 μm) or neurons treated with unconditioned medium containing LPS or IL-4 (Fig. 1D, E). This suggests that soluble factors secreted by M2-like microglia promote neurite elongation. We then examined the expression of mRNA for neurotrophic factor and cytokine in M1-like and M2-like-polarized microglia (Fig. 1F). M2-like-polarized microglia expressed a substantially higher amount of NGF mRNA. In contrast, M1-like-polarized microglia expressed increased level of TNF-α mRNA. Furthermore, the expression of TNF receptor (TNFRII) mRNA was elevated in M1-like microglial CM-treated neurons (Fig. 1G). IL-1 receptor (IL-1RI) mRNA levels also tended to be elevated in these cells (Fig. 1G).

Activated Microglia Undergo Phenotypic Switching

Microglial function may switch between the inflammatory and subsequent regenerative periods. We examined whether microglia can transform phenotypically from M1-like to M2-like in response to IL-4 and from M2-like to M1-like in response to LPS (Fig. 2). LPS increased CD86 mRNA expression in microglia (2.0 ± 0.53-fold of control). After the culture

medium was changed to the one containing IL-4, the levels of CD86 mRNA gradually declined (LPS→IL-4 24 h, 0.54 ± 0.36-fold of control) (Fig. 2B). Similar results were obtained for IL-1β (LPS→IL-4 24 h, 74.85 ± 31.64-fold of control) (Fig. 2B). In comparison, Arg1 mRNA levels were not changed after treatment with LPS, but gradually increased after the culture medium was replaced with one containing IL-4 (LPS, 0.58 ± 0.48-fold of control; LPS→IL-4 12 h, 12.76 ± 1.60-fold of control; LPS→IL-4 24 h, 12.30 ± 1.25-fold of control). Similar results were obtained for CD206 (LPS, 0.98 ± 0.47-fold of control; LPS→IL-4 24 h, 9.27 ± 2.81-fold of control) (Fig. 2B). When microglial cells were initially treated with IL-4, Arg1 mRNA levels rose, characteristic of the M2-like phenotype (IL-4, 29.0 ± 12.13-fold of control). After the culture medium was replaced with one containing LPS, Arg1 mRNA levels subsided (IL-4→LPS 12 h, 2.21 ± 0.63-fold of control) (Fig. 2B). Similar results were obtained for CD206 (IL-4→LPS 12 h, 1.32 ± 0.34-fold of control; IL-4→LPS 24 h, 2.07 ± 1.00-fold of control) (Fig. 2B). In contrast, CD86 mRNA levels rose after the change to LPS-containing medium (IL-4, 0.81 ± 0.17-fold of control; IL-4→LPS 12 h, 2.27 ± 0.26-fold of control). Similar results were obtained for IL-1β (IL-4, 1.31 ± 0.31-fold of control; IL-4→LPS 3 h, 587.20 ± 14.07-fold of control; IL-4→LPS 12 h, 1232.04 ± 74.30-fold of control) (Fig. 2B). Furthermore, we also confirmed same phenomena occurred for CCL5 and IGF-1 (Supplemental Fig. 5). Immunocytochemistry revealed that expression levels of CD86 and Arg1 changed following the change in stimulus (Fig. 2C).

We evaluated microglial morphology after the changes in stimuli (Fig. 2D–G). An 18 h LPS treatment induced an increase in soma size (area, 888.22 ± 60.96 μm^2; TI, 3.08 ± 0.32). Subsequent treatment with IL-4 induced longer processes (area, 575.06 ± 36.67 μm^2; TI, 4.24 ± 0.32). Conversely, IL-4-induced M2-like microglia (area, 451.5 ± 26.21 μm^2; TI, 6.10 ± 0.94) became round and large in response to LPS (area, 1 062.66 ± 68.02 μm^2; TI, 3.27 ± 0.44) (Fig. 2D-G). Phagocytic activity was low in LPS-treated microglia (LPS, 1.11 ± 0.19 beads), and increased following a shift to IL-4 (LPS→IL-4, 1.99 ± 0.51 beads) (Fig. 2H). The

phagocytic activity of M2-like microglia subsided after a shift from IL-4 to LPS (IL-4, 3.78 ± 0.57 beads; IL-4→LPS, 0.98 ± 0.18 beads). These results suggest that microglia have a polarization switching mechanism, and respond differentially to extracellular stimuli.

IRF7 Expression is Elevated during the M2 to M1 Switch

We subsequently sought to identify factors that control phenotypic switching in microglia. A recent study on macrophages revealed the importance of IRF4, which controls M2 macrophage polarization (Satoh et al., 2010). Other studies have shown the involvement of IRF8 in microglial activation and homeostasis (Masuda et al., 2012; Horiuchi et al., 2012). These findings suggest that microglial activation and polarization might be controlled by specific endogenous IRFs. We then examined the expression levels of IRFs in M1-like- and M2-like-polarized microglia (Fig. 3A). We found that IRF1, IRF7 and IRF9 mRNA levels increased following treatment with LPS (IRF1, 2.45 ± 0.74-fold of control; IRF7, 41.44 ± 7.21-fold of control; IRF9, 3.83 ± 0.94-fold of control), whereas IRF2 and IRF8 mRNA levels decreased after LPS treatment (IRF2, 0.40 ± 0.04-fold of control; IRF8, 0.49 ± 0.13-fold of control). In contrast, IRF4 mRNA levels increased following treatment with IL-4 (4.14 ± 1.13-fold of control). We selected the IRF7 gene and examined the expression of IRF7 mRNA with time. IRF7 mRNA was gradually increased after LPS treatment (Supplemental Fig. 6A). We also obtained similar results of the changes of IRF7 by western blotting (Supplemental Fig. 6B). We confirmed the change in IRF7 expression in microglial cell-line, BV2 (Supplemental Fig. 6B). We obtained the similar results to primary microglia although the time course was different. We next examined whether IRF7 gene responds to re-polarizing stimuli (Fig. 3B). qRT-PCR analysis revealed that IRF7 mRNA levels increased in response to LPS, as described above, and gradually decreased after the change to IL-4-containing medium (LPS→IL-4 24 h, 5.87 ± 2.21-fold of control). In contrast, IRF7 mRNA levels increased during the M2-like to M1-like polarization switch (IL-4, 1.45 ±

0.35-fold of control; IL-4→LPS 12 h, 27.43 ± 8.29-fold of control) (Fig. 3B). In the experiment of phenotypically shift from M1-like to M2-like microglia, above results raised the possibility that IL-4 induced down-regulation of IRF7 expression or IRF7 mRNA was decayed with time. We examined the expression level of IRF7 mRNA in the presence or absence of IL-4 after exchange the medium. At 24 h after the culture medium was replaced, IRF7 mRNA was decreased and its expression level was not significantly different in the presence or absence of IL-4 (LPS→IL-4 24 h, 5.86 ± 2.21-fold of control; LPS→(-) 24 h, 7.02 ± 3.18-fold of control) (Fig. 3B, left). We also examined the IRF7 mRNA expression at 3 h and 12 h (Supplemental Fig. 6C). These results suggest that IL-4 do not induce down-regulation of IRF7 mRNA expression (Supplemental Fig. 6C).

IRF7 is Associated with SCI Pathogenesis and Demyelination

It has been reported that macrophage/microglial M1 and M2 marker gene expression levels are elevated in the injured spinal cord (Kigerl et al., 2009). First, we confirmed the microglial accumulation in our SCI model (Fig. 4A). We found that mRNA levels of the M1 marker CD86, iNOS and IL-1β were elevated until 14 days post-injury, and that mRNA levels of the M2 marker Arg1, CD206 and Ym1 also rose, although the peak was earlier than that of the M1 marker, and then declined by 14 days post-injury (Fig. 4B). Immunohistochemistry revealed that CD86-positive cells were increased until 14 days post-injury (Fig. 4C). Changes in expression of IRF7 mRNA was also found. As shown in Fig. 4D, IRF7 mRNA levels were elevated until 14 days post-injury. This expression pattern was similar to that of M1 marker, indicating that IRF7 may be involved in the polarization of M1-like microglia *in vivo*. We next examined whether IRF7 was produced by microglia. Immunohistochemistry revealed that IRF7 was expressed by microglia/macrophages in the dorsal column of spinal cord at 3 and 14 days post-injury (Fig. 4E).

We next examined changes in expression of these genes in the cuprizone demyelination model. In this model, cuprizone induces demyelination in the corpus callosum without disrupting blood–brain barrier (BBB) integrity, and macrophage infiltration does not occur (Wergeland et al., 2012). Removal of cuprizone from the diet permits remyelination in this model (Matsushima and Morell, 2001). When significant demyelination was detected in this model, an increased number of microglia were observed within the lesion (Fig. 5A). We next examined mRNA expression levels of M1 and M2 markers in this model (Fig. 5B). mRNA levels of the M1-like microglial marker CD86 tended to be higher after 4 weeks of cuprizone treatment. Immunohistochemistry revealed that CD86-positive cells were increased during demyelination phase (Fig. 5C). IRF7 mRNA levels were also increased after 4 weeks on cuprizone (Fig. 5D). mRNA levels of the M2-like microglial marker Arg1 tended to be higher at the remyelination phase (2 weeks after the removal of cuprizone from the diet) (Fig. 5B). Because of individual variability in the cuprizone treatment group (Fig. 5B, D), we compared the mRNA levels of IRF7, as well as M1 and M2 markers, among individual mice. In correlation analysis, there was an association between IRF7 and CD86; however, there was only a poor correlation between IRF7 and Arg1 (Fig. 5E). This correlation suggests that an increase in IRF7-expressing microglia may be implicated in demyelination.

IRF7 Inhibition Suppresses LPS-induced M1 Marker Expression

We found that IRF7 mRNA levels were increased by LPS treatment *in vitro* (Fig. 3), and elevated in mouse models of SCI and demyelination (Figs. 4 and 5). Therefore, we examined whether reducing IRF7 expression using siRNA affects M1 marker expression *in vitro*. As a preliminary experiment, we transfected three different siRNAs against IRF7 (#1–#3) into microglia, and 30 h later, LPS was given for 18 h (Fig. 6A), and we measured IRF7 mRNA levels by qRT-PCR. We found that siRNA #3 had the strongest inhibitory effect (#2, 33.7% of control siRNA; #3, 20.6% of control siRNA) (Supplemental Fig. 7A). In the following

experiments, we used siRNA #3 to examine the role of IRF7. We next examined the expression of IRF7 in the presence of siRNA in protein level and confirmed the expression of IRF7 was suppressed by siRNA ((IRF7 siRNA, 0.60 ± 0.06-fold of control) (Supplement Fig. 7B-C). Immunocytochemistry also revealed that expression level of IRF7 was inhibited in LPS treatment (IRF7 siRNA, 64.87 ± 5.15 %) (Supplement Fig. 7D-E). IRF7 siRNA transfection reduced mRNA levels of the M1-like microglial markers induced by LPS (CD86, 0.58 ± 0.14-fold of control siRNA; iNOS, 0.56 ± 0.37-fold of control siRNA) (Fig. 6B–C, left). Additionally, while mRNA levels of the M1-like microglial markers were increased during the M2-like to M1-like shift, IRF7 siRNA suppressed these changes (CD86, 0.74 ± 0.18-fold of control siRNA; iNOS, 0.34 ± 0.13-fold of control siRNA) (Fig. 6B–C, right).

It has been shown that macrophage phenotype and activation are regulated by cytokines through the Jak-STAT signaling pathway (Hu et al., 2007). In particular, it has been reported that STAT1 is activated in response to M1 macrophage polarizing signals (Sica and Bronte 2007). We examined whether IRF7 siRNA can suppress the activation of STAT1 in microglia. When cells were treated with LPS, phosphorylation of STAT1 was detected 2 h after LPS addition (Fig. 6D). IRF7 siRNA decreased STAT1 phosphorylation (0.65 ± 0.02-fold of control siRNA) (Fig. 6E–F). This result indicates that IRF7 is involved in the STAT1-mediated M1-like microglial polarization switch.

DISCUSSION

There has been considerable debate as to whether microglial activation is favorable or unfavorable for tissue protection and repair (David and Kroner, 2011). Microglia that produce proinflammatory cytokines and contribute to tissue destruction are referred to as M1-like microglia, and microglia that produce anti-inflammatory cytokines and promote tissue repair and remodeling are termed M2-like microglia (Perry et al., 2010; Miron et al., 2013). Previous studies have shown that proinflammatory stimuli (i.e., LPS, IL-1β, TNF-α, IFN-γ) induce M1 markers in microglia, and that anti-inflammatory stimuli (i.e., IL-4, IL-10, IL-13) induce M2 markers (David and Kroner, 2011; Chhor et al., 2013; Ellert-Miklaszewska et al., 2013; Przanowski et al., 2014). LPS is reported to be the strongest inducer of M1 microglia, and the anti-inflammatory cytokine IL-4 is thought to be the strongest M2 inducer (Chhor et al., 2013). Therefore, we employed LPS and IL-4 as a proinflammatory and anti-inflammatory stimulant, respectively, in our experiments. We then examined the expression of CD86, IL-1β, CCL5 and iNOS, which are M1-like microglial markers, and the expression of Arg1, CD206 and IGF-1, which are M2-like microglial markers. CD86 triggers the proinflammatory response in macrophages/microglia (David and Kroner 2011). iNOS and Arg1 are both involved in the metabolism of L-arginine (Sica and Bronte, 2007). The chemokines are known to be differentially expressed in polarized macrophages (Montovani et al., 2004). CCL5 is induced in monocytes or macrophages in response to LPS. This chemokine produced during classical activation (M1) amplifies delayed-type hypersensitivity (DTH) reactions (Mantovani et al., 2004). iNOS is an enzyme that catalyzes the synthesis of NO and citrulline from L-arginine, and is expressed in various cells of the immune system, and its activation is considered a hallmark of M1 macrophages. In contrast, Arg1 is a manganese metalloenzyme that catalyzes the hydrolysis of L-arginine to L-ornithine and urea, and its activation is considered one of the most specific markers of M2 macrophages/microglia (Sica and Bronte, 2007; Chhor et al., 2013). Another marker of M2

macrophages/microglia are the mannose receptor (CD206) and IGF-1 (Kigerl et al., 2009; David and Kroner, 2011; Chhor et al., 2013). These markers upregulated following IL-4 stimulation. These findings led to the development of the concept of alternative activation of macrophages and microglia (Stein et al., 1992; Chhor et al., 2013). We successfully showed that these M1 markers were upregulated by LPS, and that M2 markers were upregulated by IL-4 in primary cultured microglia. Therefore, our *in vitro* system likely models well microglial activation.

The mechanisms that regulate the polarization of microglia remain unclear (Shimizu et al., 2008; Hu et al., 2012; Chhor et al., 2013). It is not clear whether M1-like and M2-like microglia are derived independently from resting state microglia, or are derived from a phenotypic shift from one form to the other. Several subpopulations of microglia are thought to exist in the CNS and may have different functions. Shimizu et al. (2008) reported that they were able to separate M1-like and M2-like microglia from heterogenous mixed glial cell cultures using different preparation methods. In contrast, a recent study found that polarized M1 and M2 macrophages/microglia can reverse phenotype in response to an external stimulus (Mosser et al., 2008; Chhor et al., 2013).

In the present study, we show that M1-like and M2-like microglia can phenotypically and functionally shift in response to extracellular factors *in vitro*. We also found differences in morphology and phagocytic activity between polarized M1-like and M2-like microglia (Fig. 1B–C and Supplemental Fig. 4). LPS-treated microglia are characterized by a large soma, while IL-4-treated microglia are characterized by long processes (Kloss et al., 2001; Zhou et al., 2012). We found a switching of microglial morphology in response to extracellular stimulus, but not all cells changed morphologically. As shown in Supplemental Fig. 4 and Fig. 2H, phagocytic activity was high in IL-4-treated microglia; however, it diminished after the shift to LPS. Phagocytic removal of damaged axons and their myelin sheaths distal to the site of injury is important for creating a favorable environment for axonal

regeneration and remyelination in the nervous system (Tanaka et al., 2009; Fu et al., 2014). The change in phagocytic activity *in vitro* in this study resembled the change *in vivo* after injury to the nervous system (Lucin and Wyss-Coray. 2009; Lucin et al., 2013).

To evaluate the effect of M1-like and M2-like microglia on neurons, we applied M1-like and M2-like microglial CM to cultured cortical neurons (Fig. 1D–E). The addition of M2-like microglial CM resulted in elongated axons. However, untreated microglial CM and M1-like microglial CM did not impact axonal growth. M1-like-polarized microglia had elevated expression of mRNAs for TNF-α and IL-1β, and M1-like microglial CM increased the expression of mRNAs for TNFRII and IL-1R1 in neurons. In contrast, M2-like-polarized microglia had elevated expression of NGF mRNA. These results suggest that M1-like microglia promote inflammation and that M2-like microglia facilitate neurite extension, in part through the production of neurotrophic factors.

A microglial polarization shift-like phenomenon was also observed *in vivo*. Kigerl et al. (2009) showed that while M1 macrophages/microglia dominate the lesion site up to 1 month after SCI, the M2 macrophage/microglial response was transient, and in most cases, returned to pre-injury levels by 7 days post-injury *in vivo*. Similar results were obtained in our SCI model (Fig. 4B-C). M1 marker CD86, iNOS and IL-1β were increased even at 14 days post-injury, while mRNA levels of the M2 marker Arg1, CD206 and Ym1 were elevated transiently. These differential patterns of gene expression suggest that functional changes in macrophages/microglia occur in the wound site.

In SCI, it is difficult to distinguish the involvement of microglia from that of macrophages. Therefore, we employed the cuprizone-induced demyelination model, which can induce demyelination without macrophage infiltration, and examined the expression levels of M1 and M2 markers (Fig. 5B-C). CD86 expression levels tended to be higher during demyelination, while mRNA levels of Arg1 tended to be higher during the remyelination phase. It is unlikely that most M1 microglia disappear and newly formed M2 cells migrate

into the demyelinated lesion. Therefore, we consider that our findings provide indirect evidence of phenotypic switching in microglia.

A recent study on macrophages revealed the importance of IRF4, which controls M2 macrophage polarization (Satoh et al., 2010). Another study showed that M1 macrophages upregulate IRF5, which is essential for the induction of cytokines involved in eliciting Th1 and Th17 responses (Krausgruber et al., 2011). In addition to the important roles of IRFs in macrophages, IRF8 has been shown to play a role in adult microglial homeostasis and activation (Horiuchi et al., 2012, Masuda et al., 2012). The IRF family has now expanded to nine members (IRF1–IRF9), and critical roles of these members in multiple processes have been shown (Takaoka et al., 2008). Therefore, we examined the expression of mRNAs for IRFs because they are endogenous factors related to microglial activation. In this study, we found that IRF7 expression was most similar to that of M1 markers *in vitro* (Fig. 3A), and that expression changed in response to extracellular stimuli (Fig. 3B). It has been demonstrated that IRF7 is expressed at low levels and is induced by Toll-like receptor (TLR) 4 signaling (Takaoka et al., 2008). The expression of IRF7 mRNA changed *in vivo* as well. After SCI, IRF7 displayed an expression pattern similar to that of M1 markers (Fig. 4). In the cuprizone model, the change in IRF7 mRNA expression tended to be similar to CD86 mRNA expression, but the changes were not statistically significant (Fig. 5B, D). This lack of significance may be because of concomitant demyelination / remyelination and overlapping de- and remyelination or variable response among individual animals. We therefore performed correlational analysis for IRF7 and M1 (CD86) or M2 (Arg1) marker mRNAs. IRF7 mRNA expression showed correlation with CD86 mRNA expression, suggestive of their inflammatory roles in vivo. Khorooshi et al. (2010) showed that injury to the brain upregulates expression of IRF7 and related inflammatory factors in a similar time course. Interestingly, Salem et al. (2011) showed an association between IRF7 and clinical score in experimental autoimmune encephalomyelitis, suggesting a role of the factor in inflammation.

Our present findings show an involvement of IRF7 in demyelination. However, a role in remyelination still remains to be investigated.

IRF7 siRNA suppressed the expression of mRNAs for CD86 and iNOS in M1-like-polarized microglia and during the M2-like to M1-like microglial shift (Fig. 6B–C). Moreover, phosphorylation of STAT1 was decreased by IRF7 siRNA (Fig. 6E–F). These results suggest that IRF7 contributes to STAT1-mediated M1-like microglial polarization. It has been reported that IRF7 gene is induced by IFNs through activation of the Jak-STAT pathway and ISGF3 (IFN-stimulated gene factor 3) transcription factor (Marié et al., 1998), and IRF7 is a key factor in the positive feedback regulation of IFN-α/β production (Sato et al., 1998; Honda et al., 2005). It was also shown in a model of axonal degeneration that IRF7 as well as other IFN stimulated genes are upregulated in microglia (Hosmane et al., 2012; Owens et al., 2014). Indeed, we confirmed that LPS induced the IFN-β and IRF7 siRNA suppressed the expression of IFN-β mRNA in microglia (Supplement Fig. 7F-G). In murine microglial cultures, Przanowski et al. (2014) reported that LPS induces STAT1 activation at 1.5 h. We also confirmed that LPS lead to the onset of IRF7 expression at 1 h (Supplement Fig. 6B). These data suggest that IRF7 might be function as positive feedback regulation of type I IFN and regulate the subsequent M1 marker expression in microglia. However, IRF7 siRNA did not affect the expression of another M1 marker, IL-1β (Supplemental Fig. 7H), suggesting that IRF7 does not regulate expression of every M1 marker. Nonetheless, taken together, our findings suggest an important role of IRF7 in microglial phenotypic switching. IRF7 may be a promising therapeutic target for neurodegenerative diseases associated with demyelination.

SUPPORTING INFORMATION

Additional supporting information may be found in the online version of this article at the publisher’s website.

ACKNOWLEDGMENTS

We thank Dr. J Tanaka (Ehime University), Dr. H Konishi (Nagoya University), and Mr. K Hazawa for technical assistance. This work was supported by a Grant-in-Aid for Young Scientists (B) (to T. T.) and by the Uehara Memorial Foundation (to T.T.).

REFERENCES

Ajmone-Cat MA, Mancini M, De Simone R, Cilli P, Minghetti L. 2013. Microglial polarization and plasticity: evidence from organotypic hippocampal slice cultures. Glia. 61: 1698-1711.

Beutner C, Linnartz-Gerlach B, Schmidt SV, Beyer M, Mallmann MR, Staratschek-Jox A, Schultze JL, Neumann H. 2013. Unique transcriptome signature of mouse microglia. Glia. 61: 1429-1442.

Biber K, Owens T, Boddeke E. 2014. What is microglia neurotoxicity (Not)? Glia. 62: 841-854.

Bouhlel MA, Derudas B, Rigamonti E, Dièvart R, Brozek J, Haulon S, Zawadzki C, Jude B, Torpier G, Marx N, Staels B, Chinetti-Gbaguidi G. 2007. PPARgamma activation primes human monocytes into alternative M2 macrophages with anti-inflammatory properties. Cell Metab. 6: 137-143.

Butovsky O, Jedrychowski MP, Moore CS, Cialic R, Lanser AJ, Gabriely G, Koeglsperger T, Dake B, Wu PM, Doykan CE, Fanek Z, Liu L, Chen Z, Rothstein JD, Ransohoff RM, Gygi SP, Antel JP, Weiner HL. 2014. Identification of a unique TGF-β-dependent molecular and functional signature in microglia. Nat Neurosci 17: 131-143.

Chhor V, Le Charpentier T, Lebon S, Oré MV, Celador IL, Josserand J, Degos V, Jacotot E, Hagberg H, Sävman K, Mallard C, Gressens P, Fleiss B. 2013. Characterization of phenotype markers and neuronotoxic potential of polarised primary microglia in vitro. Brain Behav Immun 32: 70-85.

David S and Kroner A. 2011. Repertoire of microglial and macrophage responses after spinal cord injury. Nat Rev Neurosci 12: 388-399.

Durafourt BA, Moore CS, Zammit DA, Johnson TA, Zaguia F, Guiot MC, Bar-Or A, Antel JP. 2012. Comparison of polarization properties of human adult microglia and blood-derived macrophages. Glia. 60: 717-727.

Ellert-Miklaszewska A, Dabrowski M, Lipko M, Sliwa M, Maleszewska M, Kaminska B. 2013. Molecular definition of the pro-tumorigenic phenotype of glioma-activated microglia. Glia. 61: 1178-1190.

Fu R, Shen Q, Xu P, Luo JJ, Tang Y. 2014. Phagocytosis of microglia in the central nervous system diseases. Mol Neurobiol 49: 1422-1434.

Fujita H, Tanaka J, Toku K, Tateishi N, Suzuki Y, Matsuda S, Sakanaka M, Maeda N. 1996. Effects of GM-CSF and ordinary supplements on the ramification of microglia in culture: a morphometrical study. Glia 18: 269-281.

Ginhoux F, Greter M, Leboeuf M, Nandi S, See P, Gokhan S, Mehler MF, Conway SJ, Ng LG, Stanley ER, Samokhvalov IM, Merad M. 2010. Fate mapping analysis reveals that adult microglia derive from primitive macrophages. Science 330: 841-845.

Hanisch UK and Kettenmann H. 2007. Microglia: active sensor and versatile effector cells in the normal and pathologic brain. Nat Neurosci 10: 1387-1394.

Honda K, Yanai H, Negishi H, Asagiri M, Sato M, Mizutani T, Shimada N, Ohba Y, Takaoka A, Yoshida N, Taniguchi T. 2005. IRF-7 is the master regulator of type-I interferon-dependent immune responses. Nature. 434: 772-777.

Horiuchi M, Wakayama K, Itoh A, Kawai K, Pleasure D, Ozato K, Itoh T. 2012. Interferon regulatory factor 8/interferon consensus sequence binding protein is a critical transcription factor for the physiological phenotype of microglia. J Neuroinflammation 9: 227.

Hosmane S, Tegenge MA, Rajbhandari L, Uapinyoying P, Kumar NG, Thakor N, Venkatesan A. 2012. Toll/interleukin-1 receptor domain-containing adapter inducing interferon-β mediates microglial phagocytosis of degenerating axons. J Neurosci. 32: 7745-7757.

Hu X, Chen J, Wang L, Ivashkiv LB. 2007. Crosstalk among Jak-STAT, Toll-like receptor, and ITAM-dependent pathways in macrophage activation. J Leukoc Biol 82: 237-243.

Hu X, Li P, Guo Y, Wang H, Leak RK, Chen S, Gao Y, Chen J. 2012. Microglia/macrophage polarization dynamics reveal novel mechanism of injury expansion after focal cerebral ischemia. Stroke 43: 3063-3070.

Jenkins SJ, Ruckerl D, Cook PC, Jones LH, Finkelman FD, van Rooijen N, MacDonald AS, Allen JE. 2011. Local macrophage proliferation, rather than recruitment from the blood, is a signature of TH2 inflammation. Science 332: 1284-1288.

Khorooshi R and Owens T. 2010. Injury-induced type I IFN signaling regulates inflammatory responses in the central nervous system. J Immunol 185: 1258-1264.

Kigerl KA, Gensel JC, Ankeny DP, Alexander JK, Donnelly DJ, Popovich PG. 2009. Identification of two distinct macrophage subsets with divergent effects causing either neurotoxicity or regeneration in the injured mouse spinal cord. J Neurosci 29: 13435-13444.

Kloss CU, Bohatschek M, Kreutzberg GW, Raivich G. 2001. Effect of lipopolysaccharide on the morphology and integrin immunoreactivity of ramified microglia in the mouse brain and in cell culture. Exp Neurol 168: 32-46.

Krausgruber T, Blazek K, Smallie T, Alzabin S, Lockstone H, Sahgal N, Hussell T, Feldmann M, Udalova IA. 2011. IRF5 promotes inflammatory macrophage polarization and TH1-TH17 responses. Nat Immunol 12: 231-238.

Liu YC, Zou XB, Chai YF, Yao YM. 2014. Macrophage polarization in inflammatory diseases. Int. J. Biol Sci.10: 520-529.

Lucin KM, O'Brien CE, Bieri G, Czirr E, Mosher KI, Abbey RJ, Mastroeni DF, Rogers J, Spencer B, Masliah E, Wyss-Coray T. 2013. Microglial beclin 1 regulates retromer trafficking and phagocytosis and is impaired in Alzheimer’s disease. Neuron 79: 873-886.

Lucin KM and Wyss-Coray T. 2009. Immune activation in brain aging and neurodegeneration: too much or too little? Neuron 64: 110-122.

Mantovani A, Sica A, Sozzani S, Allavena P, Vecchi A, Locati M. 2004. The chemokine system in diverse forms of macrophage activation and polarization. Trends Immunol. 25: 677-686.

Marié I, Durbin JE, Levy DE. 1998. Differential viral induction of distinct interferon-alpha genes by positive feedback through interferon regulatory factor-7. EMBO J. 17: 6660-6669.

Masuda T, Tsuda M, Yoshinaga R, Tozaki–Saitoh H, Ozato K, Tamura T, Inoue K. 2012. IRF8 is a critical transcription factor for transforming microglia into a reactive phenotype. Cell Rep 1: 334-340.

Matsushima GK and Morell P. 2001. The neurotoxicant, cuprizone, as a model to study demyelination and remyelination in the central nervous system. Brain Pathol 11: 107-116.

Melief J, Koning N, Schuurman KG, Van De Garde MD, Smolders J, Hoek RM, Van Eijk M, Hamann J, Huitinga I. 2012. Phenotyping primary human microglia: tight regulation of LPS responsiveness. Glia. 60: 1506-1517.

Miron VE, Boyd A, Zhao JW, Yuen TJ, Ruckh JM, Shadrach JL, van Wijngaarden P, Wagers AJ, Williams A, Franklin RJ, ffrench-Constant C. 2013. M2 microglia and macrophages drive oligodendrocyte differentiation during CNS remyelination. Nat Neurosci 16: 1211-1218.

Mosser DM, Edwards JP. 2008. Exploring the full spectrum of macrophage activation. Nat Rev Immunol 8: 958-969.

Murakami K, Jiang YP, Tanaka T, Bando Y, Mitrovic B, Yoshida S. 2013. In vivo analysis of kallikrein-related peptidase 6 (KLK6) function in oligodendrocyte development and the expression of myelin proteins. Neuroscience 236: 1-11.

Olah M, Amor S, Brouwer N, Vinet J, Eggen B, Biber K, Boddeke HW. 2012. Identification of a microglia phenotype supportive of remyelination. Glia. 60: 306-321.

Owens T, Khorooshi R, Wlodarczyk A, Asgari N. 2014. Interferons in the central nervous system: a few instruments play many tunes. Glia. 62: 339-355.

Perry VH, Nicoll JA, Holmes C. 2010. Microglia in neurodegenerative disease. Nat Rev Neurol 6: 193-201.

Przanowski P, Dabrowski M, Ellert-Miklaszewska A, Kloss M, Mieczkowski J, Kaza B, Ronowicz A, Hu F, Piotrowski A, Kettenmann H, Komorowski J, Kaminska B. 2014. The signal transducers Stat1 and Stat3 and their novel target Jmjd3 drive the expression of inflammatory genes in microglia. J Mol Med (Berl). 92: 239-254.

Saijo K and Glass CK. 2011. Microglial cell origin and phenotypes in health and disease. Nat Rev Immunol 11: 775-787.

Salem M, Mony JT, Løbner M, Khorooshi R, Owens T. 2011. Interferon regulatory factor-7 modulates experimental autoimmune encephalomyelitis in mice. J Neuroinflammation 8: 181.

Sato M, Hata N, Asagiri M, Nakaya T, Taniguchi T, Tanaka N. 1998. Positive feedback regulation of type I IFN genes by the IFN-inducible transcription factor IRF-7. FEBS Lett. 441: 106-110.

Satoh T, Takeuchi O, Vandenbon A, Yasuda K, Tanaka Y, Kumagai Y, Miyake T, Matsushita K, Okazaki T, Saitoh T, Honma K, Matsuyama T, Yui K, Tsujimura T, Standley DM, Nakanishi K, Nakai K, Akira S. 2010. The Jmjd3-Irf4 axis regulates M2 macrophage polarization and host responses against helminth infection. Nat Immunol 11: 936-944.

Schmid CD, Melchior B, Masek K, Puntambekar SS, Danielson PE, Lo DD, Sutcliffe JG, Carson MJ. 2009. Differential gene expression in LPS/IFNgamma activated microglia and macrophages: in vitro versus in vivo. J Neurochem 109: 117-125.

Shimizu E, Kawahara K, Kajizono M, Sawada M, Nakayama H. 2008. IL-4-induced selective clearance of oligomeric β-amyloid peptide1-42 by rat primary type 2 microglia. J Immunol 181: 6503-6513.

Sica A, Bronte V. 2007. Altered macrophage differentiation and immune dysfunction in tumor development. J Clin Invest 117: 1155-1166.

Sica A and Mantovani A. 2012. Macrophage plasticity and polarization: in vivo veritas. J Clin Invest. 122: 787-795.

Stein M, Keshav S, Harris N, Gordon S. 1992. Interleukin 4 potently enhances murine macrophage mannose receptor activity: a marker of alternative immunologic macrophage activation. J Exp Med 176: 287-292.

Takaoka A, Tamura T, Taniguchi T. 2008. Interferon regulatory factor family of transcription factors and regulation of oncogenesis. Cancer Sci 99: 467-478.

Tanaka T, Murakami K, Bando Y, Yoshida S. 2013. Minocycline reduces remyelination by suppressing ciliary neurotrophic factor expression after cuprizone-induced demyelination. J Neurochem 127: 259-270.

Tanaka T, Ueno M, Yamashita T. 2009. Engulfment of axon debris by microglia requires p38 MAPK activity. J Biol Chem 284: 21626–21636.

Ueno M, Fujita Y, Tanaka T, Nakamura Y, Kikuta J, Ishii M, Yamashita T. 2013. Layer V cortical neurons require microglial support for survival during postnatal development. Nat Neurosci 16: 543-551.

Wang G, Zhang J, Hu X, Zhang L, Mao L, Jiang X, Liou AK, Leak RK, Gao Y, Chen J. 2013. Microglia/macrophage polarization dynamics in white matter after traumatic brain injury. J Cereb Blood Flow Metab 33: 1864-1874.

Wergeland S, Torkildsen Ø, Myhr KM, Mørk SJ, Bø L. 2012. The cuprizone model: regional heterogeneity of pathology. APMIS 120: 648-657.

Zhou X, Spittau B, Krieglstein K. 2012. TGFβ signalling plays an important role in IL4-induced alternative activation of microglia. J Neuroinflammation 9: 210.

FIGURE LEGENDS

FIGURE 1: Characterization of M1-like and M2-like microglial phenotypes. **A**: Expression profile of mRNA for M1-like microglial markers (CD86 and IL-1β) and M2 markers (Arg1 and CD206) following treatment with LPS or IL-4 for 18 h. Data are presented as the mean ± SEM of three or four independent experiments. **P* < 0.05, ***P* < 0.01 compared with control. **B**: Microglial morphological changes in response to LPS or IL-4. Representative immunocytochemical labeling for Iba1 in microglial cells after 12 h treatment with LPS or IL-4. Scale bar, 20 μm. **C**: Quantification of cell "roundness" in M1-like and M2-like microglial cells. Relationship between the perimeter of the microglial cell and its cell area was plotted. LPS or IL-4 was administered for 12 h. TI values were calculated as [perimeter of cell (μm)]^2/4π [cell area (μm^2)]. **D**: Representative immunocytochemical labeling for Tuj1 in cortical neurons treated with microglial conditioned media (CM) for 48 h. CM (con), CM of control microglial cells; CM (LPS), CM of LPS-treated microglial cells; CM (IL-4), CM of IL-4-treated microglial cells; unCM, neurons cultured with unconditioned medium; unCM+LPS, neurons cultured with unconditioned medium and LPS; unCM+IL-4, neurons cultured with unconditioned medium and IL-4. Scale bar, 200 μm. **E**: Quantification of axon length in CM-treated and unCM-treated neurons. **F**: Expression profile of mRNAs for neurotrophic factor and cytokine in M1-like- and M2-like-polarized microglia. Data are presented as the mean ± SEM of three to five independent experiments. **P* < 0.05, ***P* < 0.01. **G**: Expression profile of cytokine receptor mRNAs in M1-like- or M2-like-polarized microglial CM-treated neurons. Data are presented as the mean ± SEM of three independent experiments. **P* < 0.05, ***P* < 0.01 compared with control.

FIGURE 2: M1-like and M2-like microglial profiles switch in response to IL-4 and LPS. **A**: Diagram of the scheme of LPS and IL-4 treatment. Microglial cells were first cultured with

LPS or IL-4 for 18 h, and the medium was exchanged with one containing IL-4 or LPS, respectively, for the indicated time. **B**: Expression profiles of CD86, IL-1β, Arg1 and CD206 mRNAs during the M1-like to M2-like or M2-like to M1-like microglial shift. (−) denotes that microglia were treated with LPS or IL-4 for 18 h and then cells were exposed to new medium without stimulant. Data are presented as the mean ± SEM of three independent experiments. *P < 0.05, **P < 0.01. **C**: Representative immunocytochemical labeling for CD86 (green) and Arg1 (red) during the microglial polarization shift. We treated microglia with LPS or IL-4 for 18 h and then exchanged the medium for one containing IL-4 or LPS for 12 h. Scale bar, 100 μm. **D**: Relationship between the perimeter of the microglial cell and its cell area after the polarization shift. Parameters were measured 12 h after the medium exchange. **E**: Cell area of microglial cells at the time points described in C. Data are presented as the mean ± SEM of seven independent experiments. **P < 0.01. **F**: Transformation index (TI) of microglial cells at the time points described in C. TI values were calculated as [perimeter of cell (μm)]^2/4π [cell area (μm^2)]. Data are presented as the mean ± SEM of seven independent experiments. *P < 0.05, **P < 0.01. **G**: Representative immunocytochemical labeling for Iba1 (red) in microglia. Scale bar, 20 μm. **H**: Phagocytic assay during the M1-like to M2-like or M2-like to M1-like microglial shift. Microspheres were given for 1 h. Data are presented as the mean ± SEM of four independent experiments. *P < 0.05, **P < 0.01.

FIGURE 3: IRF7 expression is elevated in M1-like microglia. **A**: Microglial cells were cultured with the indicated factors for 18 h and subjected to qRT-PCR. The relative amounts to control cultures are shown. Data are presented as the mean ± SEM of three to seven independent experiments. *P < 0.05, **P < 0.01 compared with control. **B**: Expression profile of IRF7 mRNA during the M1-like to M2-like or M2-like to M1-like microglial shift. Microglial cells were first cultured with LPS or IL-4 for 18 h and the medium was exchanged

with one containing IL-4 or LPS, respectively, for the indicated hours. (−) denotes that microglia were treated with LPS or IL-4 for 18 h and then cells were exposed to new medium without stimulant. N.S., not significantly different. Data are presented as the mean ± SEM of three independent experiments. *$P < 0.05$.

FIGURE 4: Spinal cord injury induces changes in the expression of microglial polarization genes. **A**: Confocal images of the dorsal column of spinal cord at the lesion epicenter stained for Iba1 (red) and DAPI (blue). Images were taken from the red-boxed area. Scale bar, 50 μm. dpi, days post-injury. **B**: Expression profile of factors associated with M1-like (CD86, iNOS and IL-1β) and M2-like (Arg1, CD206 and Ym1) microglia/macrophages in the injured spinal cord. Expressions relative to that in the intact spinal cord are shown. Data are presented as the mean ± SEM of three or four independent experiments. *$P < 0.05$, **$P < 0.01$ compared with the intact cord. **C**: Confocal images of the dorsal column of spinal cord stained for CD86 (red) and DAPI (blue). **D**: Expression profile of IRF7 mRNA in the damaged spinal cord. Data are presented as the mean ± SEM of three or four independent experiments. *$P < 0.05$, **$P < 0.01$ compared with the intact cord. **E**: Confocal images of the dorsal column of spinal cord stained for ED1 (CD68) (green) and IRF7 (red). Scale bar, 50 μm.

FIGURE 5: Involvement of microglial activation in cuprizone-induced demyelination. **A**: Images were taken from the red-boxed area. Confocal images of the corpus callosum of cuprizone-treated mice stained for Iba1 (red) and DAPI (blue). Con, control; c4w, 4 weeks of cuprizone treatment; c4w+n2w, 4 weeks of cuprizone treatment and following 2 weeks of normal diet. Scale bar, 50 μm. **B**: Expression profile of mRNAs associated with M1 (CD86) and M2 (Arg1) microglia in demyelination (c4w, cuprizone 4 weeks) and remyelination (c4w + n2w, cuprizone 4 weeks and normal diet 2 weeks). The relative amounts to control are

shown. Data are presented as the mean ± SEM. n = 4 to 5 animals per group. **C**: Confocal images of the corpus callosum of cuprizone-treated mice stained for CD86 (red) and DAPI (blue). Scale bar, 50 μm. **D**: Expression profile of IRF7 mRNA in cuprizone-treated mice. Data are presented as the mean ± SEM. n = 4 to 5 animals per group. **E**: Correlation between IRF7 and M1/M2 marker genes (CD86, Arg1) in cuprizone-induced demyelination from mice (n = 20) at control, demyelination phase (cuprizone 3w, 4w) and remyelination phase (cuprizone 4w + normal diet 1w, 2w).

FIGURE 6: Knockdown of IRF7 by siRNA suppress LPS-induced M1 marker expressions. **A**: Diagram of the scheme of transfection of siRNA. After 30 h of transfection, the cells were treated with LPS or IL-4. **B, C**: Expression profile of CD86 and iNOS mRNAs in M1 microglia (left) or during the M2 to M1 microglial shift (right). For polarization switching, microglial cells were first cultured with IL-4 for 18 h and the medium was exchanged with one containing LPS for 12 h. Data are presented as the mean ± SEM of three to five independent experiments. $*P < 0.05$. **D**: Western blot analysis of STAT1 phosphorylation in microglia. Cells were treated with LPS for up to 2 h, and then, cell lysates were prepared and subjected to immunoblotting with anti-phospho-STAT1 and anti-STAT1 antibodies. **E**: Western blot analysis of STAT1 phosphorylation in IRF7 siRNA-transfected microglia. Microglial cells were cultured with LPS for 2 h. **F**: Quantification of the density of the phosphorylation level of STAT1. Data are presented as the mean ± SEM of three independent experiments. $*P < 0.05$.

Supporting information

Interferon regulatory factor 7 participates in the M1-like microglial polarization switch

Tatsuhide Tanaka[†], Koichi Murakami, Yoshio Bando and Shigetaka Yoshida

Department of Functional Anatomy and Neuroscience, Asahikawa Medical University, Midorigaoka-higashi 2-1-1-1 Asahikawa, Hokkaido 078-8510, Japan

[†]**Corresponding author:**

Tatsuhide Tanaka

Tel.: +81-166-68-2303; Fax: +81-166-68-2309; E-mail: ttanaka@asahikawa-med.ac.jp

Supplementary Figure legends

Figure S1. LPS and IL-4 change mRNA expression of M1 and M2 polarization markers, respectively. **A**: Expression profile of mRNA for M1-like microglial markers (CCL5, IL-6, iNOS and CXCL1) and M2 markers (IGF1 and PPARγ) following treatment with LPS or IL-4 for 18 h. Data are presented as the mean ± SEM of three or four independent experiments. $*P < 0.05$, $**P < 0.01$ compared with control. **B**: Representative immunocytochemical labeling for CD86 (green) and Arg1 (red) in LPS- or IL-4-treated microglial cells. Cells were treated for 18 h with each reagent. Scale bar, 100 μm.

Figure S2. Changes in microglial morphology in response to LPS or IL-4 stimulation at the indicated time. Representative micrographs and drawings for quantification of TI indices are shown. Scale bar, 30 μm.

Figure S3. Microglial morphology in primary cultures. **A**: Representative immunocytochemical labeling for Iba1. We treated microglia with LPS or IL-4 for 12 h. Scale bar, 50 μm. Group A: Microglial cells with small round or slightly ovoid somata. Group B: Microglial cells with larger somata and a few processes. Group C: Microglial cells with asymmetric or rod-shaped somata and long processes. **B**: Quantitative analysis of microglial morphology after polarization into the M1 or M2 type.

Figure S4. Phagocytic assay in M1-like- or M2-like-polarized microglia. **A**: Diagram of the scheme of fluorescent latex bead treatment. **B**: Representative labeling for Iba1 (red) and fluorescent latex beads (green). Scale bar, 100 μm. Lower panels, higher magnification image of each treated microglial cell.

Figure S5. Expression profiles of CCL5 and IGF-1 mRNAs during the M1-like to M2-like or M2-like to M1-like microglial shift. (−) denotes that microglia were treated with LPS or IL-4 for 18 h and then cells were exposed to new medium without stimulant. Data are presented as the mean ± SEM of three independent experiments. $^{**}P < 0.01$.

Figure S6. Expression level of IRF7 mRNA and protein in microglia. **A**: Expression profile of IRF7 mRNA in LPS-stimulated microglia. Data are presented as the mean ± SEM of three independent experiments. **B**: Expression profile of IRF7 protein in primary cultured microglia and microglial cell-line, BV2. **C**: Expression profile of IRF7 mRNA during the M1-like to M2-like microglial shift. Microglial cells were first cultured with LPS for 18 h and the medium was exchanged with one

containing IL-4 for the indicated hours (3 or 12 h). (−) denotes that microglia were treated with LPS for 18 h and then cells were exposed to new medium without stimulant. N.S., not significantly different. Data are presented as the mean ± SEM of three independent experiments.

Figure S7. Effect of IRF7 siRNA on M1 marker expression. **A**: Expression profile of IRF7 mRNA in microglia treated with LPS or transfected with IRF7 siRNA (#1–#3). Microglial cells were cultured with LPS for 18 h. Data are presented as the mean ± SEM of three independent experiments. *$P <$ 0.05. **B**: Western blot analysis of IRF7 in IRF7 siRNA-transfected microglia. Microglial cells were cultured with LPS for 18 h. **C**: Quantification of the density of the expression level of IRF7. Data are presented as the mean ± SEM of three independent experiments. *$P < 0.05$. **D**: Representative immunocytochemical labeling for ED1 (green) and IRF7 (red) in IRF7 siRNA-transfected microglia. Microglial cells were cultured with LPS for 18 h. Scale bar, 50 μm. **E**: Quantification of the density of the expression level of IRF7. Data are presented as the mean ± SEM of three independent experiments. *$P < 0.05$. **F**: Expression profile of IFN-β mRNA in microglia treated with LPS. Microglial cells were cultured with LPS for 18 h. Data are presented as the mean ± SEM of three independent experiments. *$P < 0.05$. **G**: Expression profile of IFN-β mRNA in M1-like microglia (left) or during the M2-like to M1-like shift (right). Data are presented as the mean ± SEM of three to three independent experiments. **H**: Expression profile of IL-1β mRNA in M1-like microglia (left) or during the M2-like to M1-like shift (right). For polarization switching, microglial cells were first cultured with IL-4 for 18 h and the medium was exchanged with one containing LPS for 12 h. N.S., not significantly different. Data are presented as the mean ± SEM of three to five independent experiments.

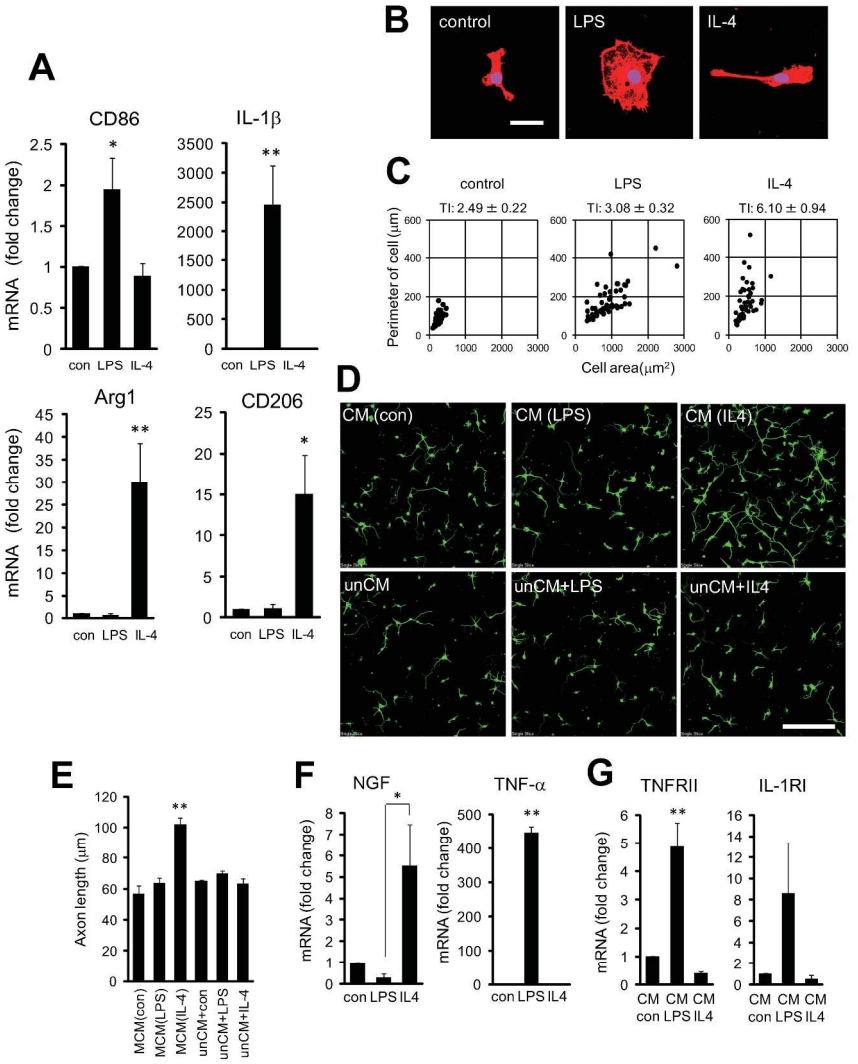

Fig. 1 Tanaka *et al.*

273x383mm (300 x 300 DPI)

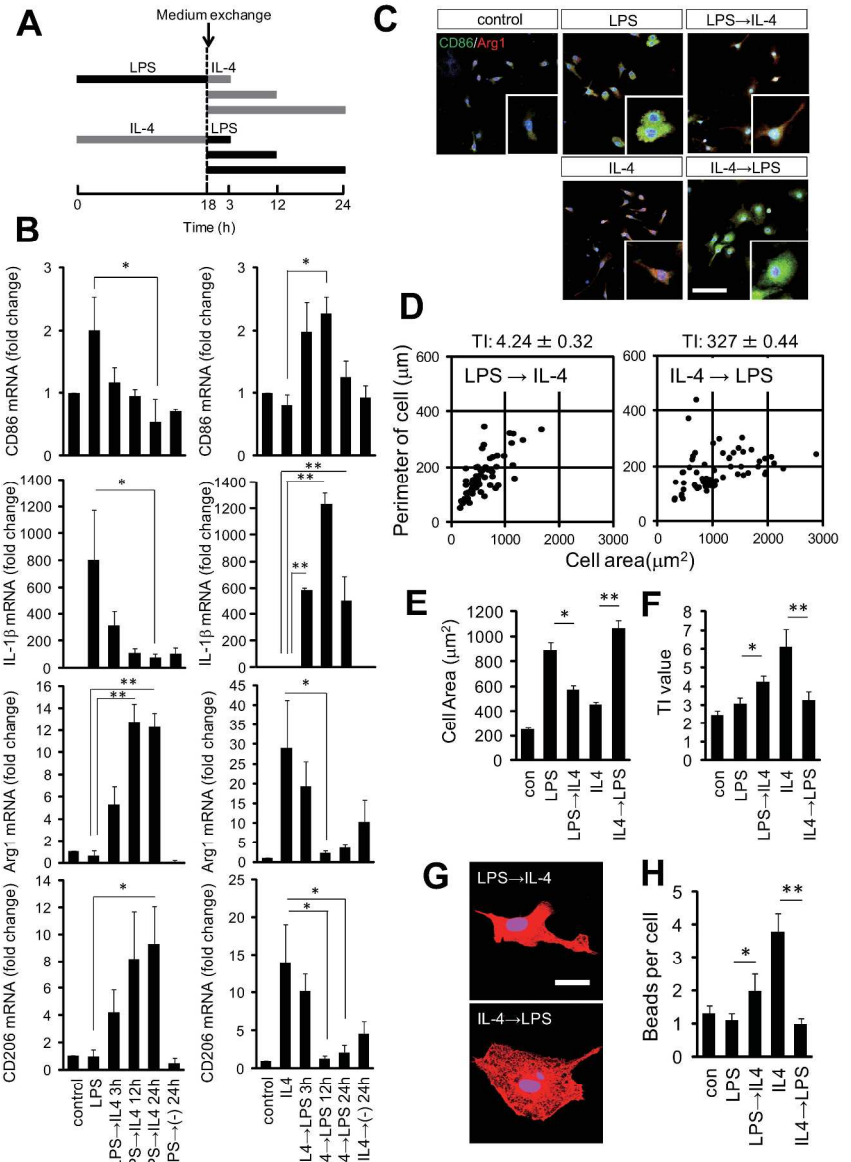

Fig. 2 Tanaka *et al.*

281x397mm (300 x 300 DPI)

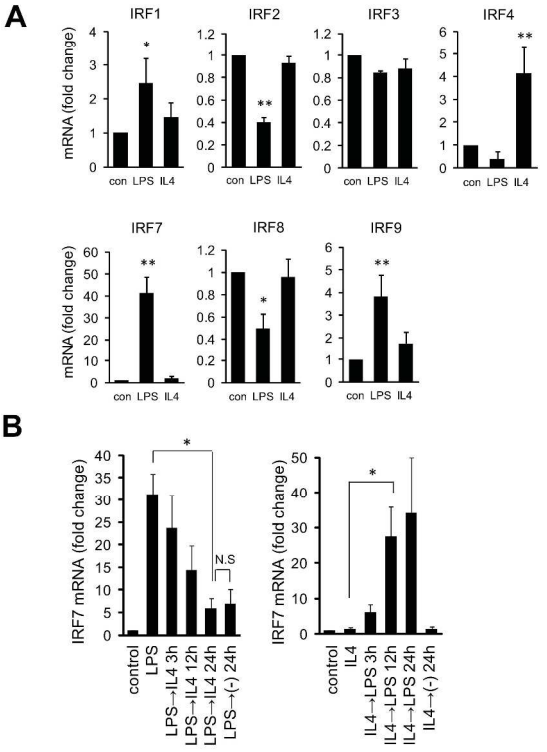

Fig. 3 Tanaka *et al.*

334x627mm (300 x 300 DPI)

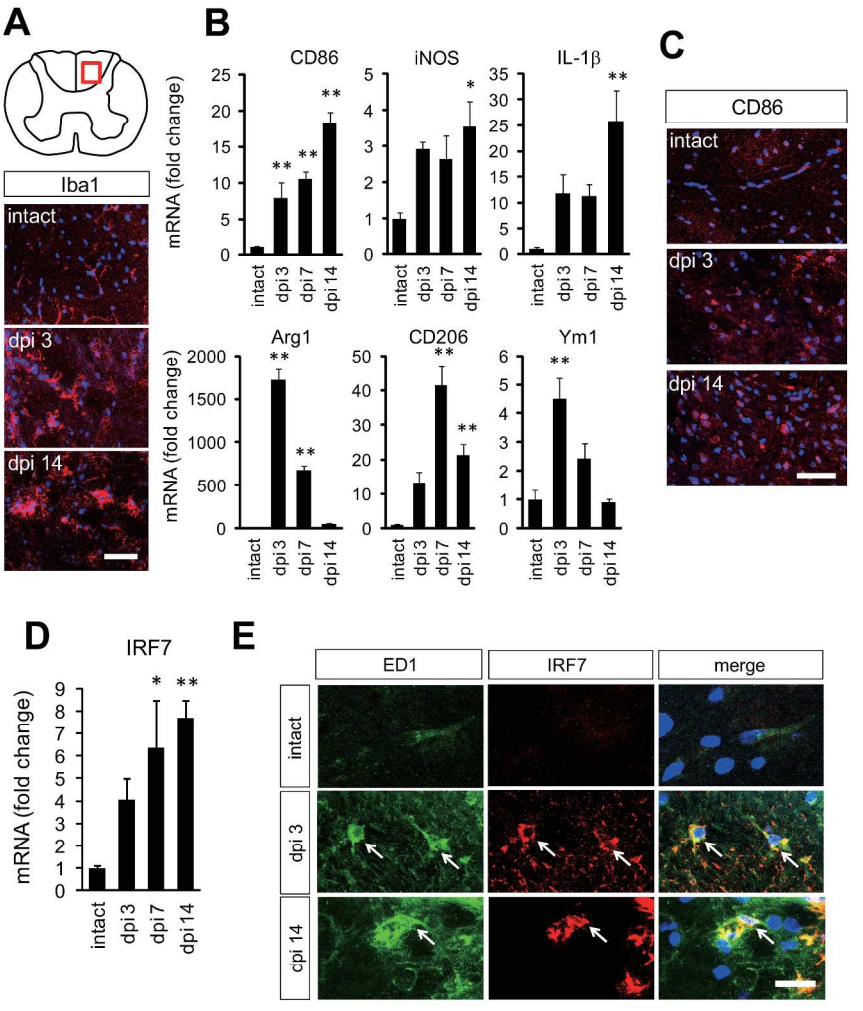

Fig. 4 Tanaka *et al.*

266x378mm (300 x 300 DPI)

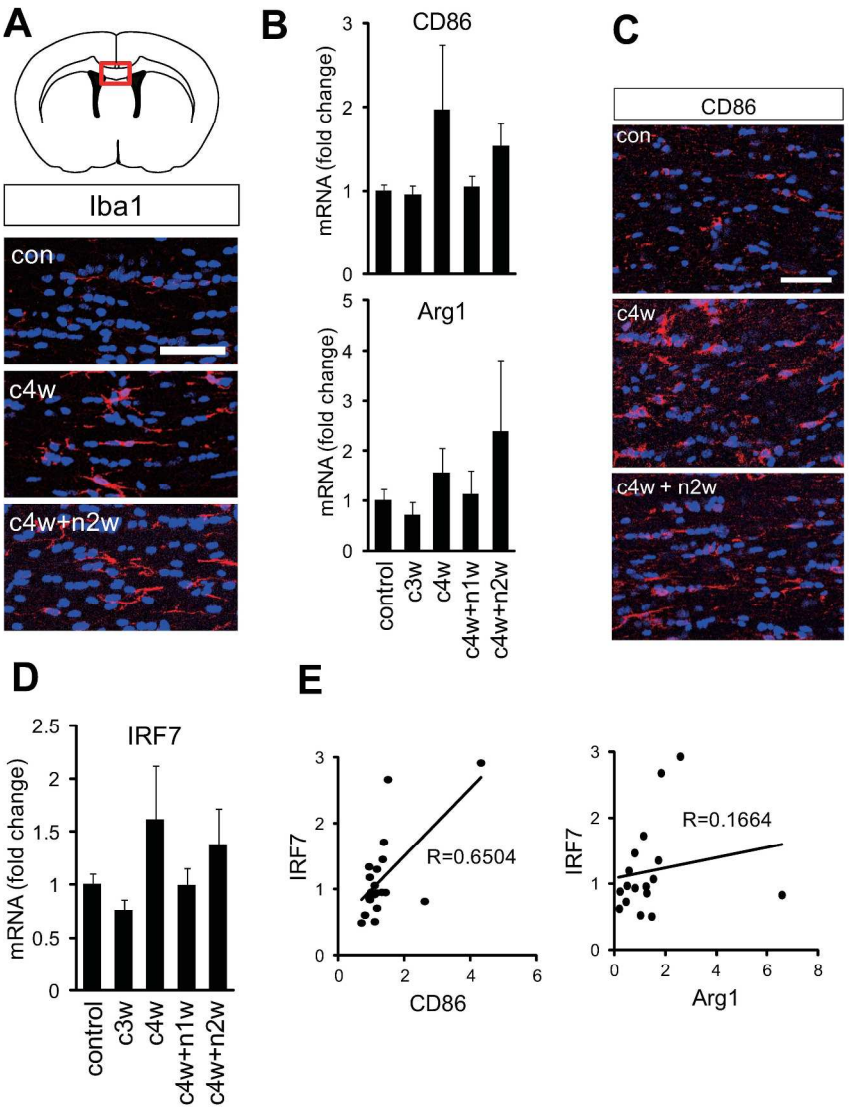

Fig. 5 Tanaka *et al.*

254x347mm (300 x 300 DPI)

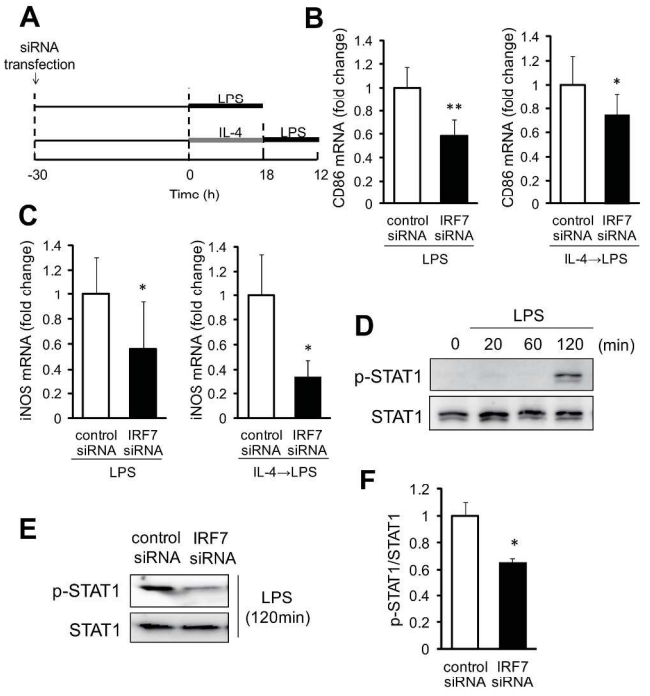

Fig. 6 Tanaka *et al.*

258x223mm (300 x 300 DPI)

Supplementary Fig. 1

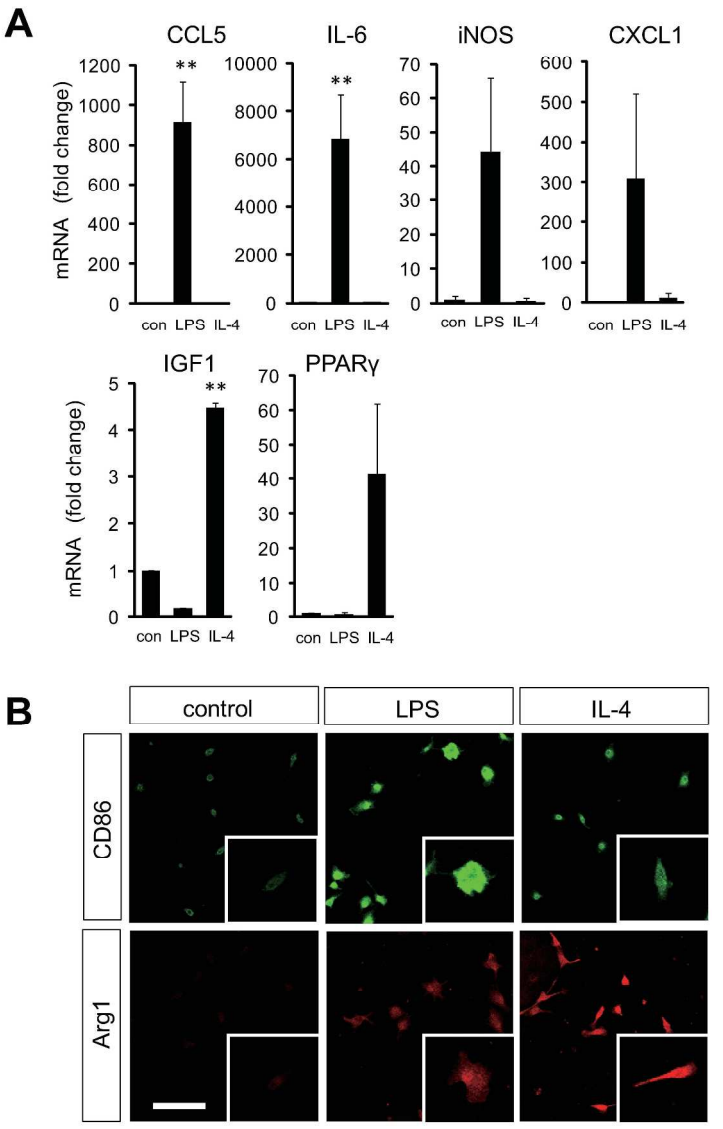

257x421mm (300 x 300 DPI)

Supplementary Fig. 2

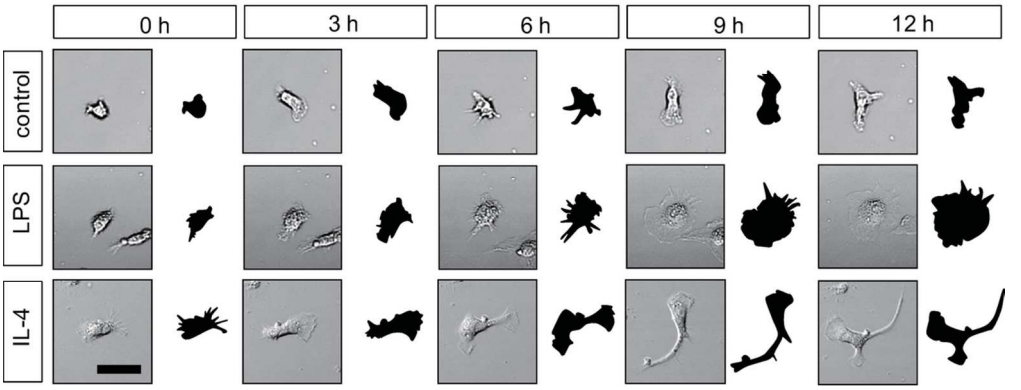

105x65mm (300 x 300 DPI)

Supplementary Fig. 3

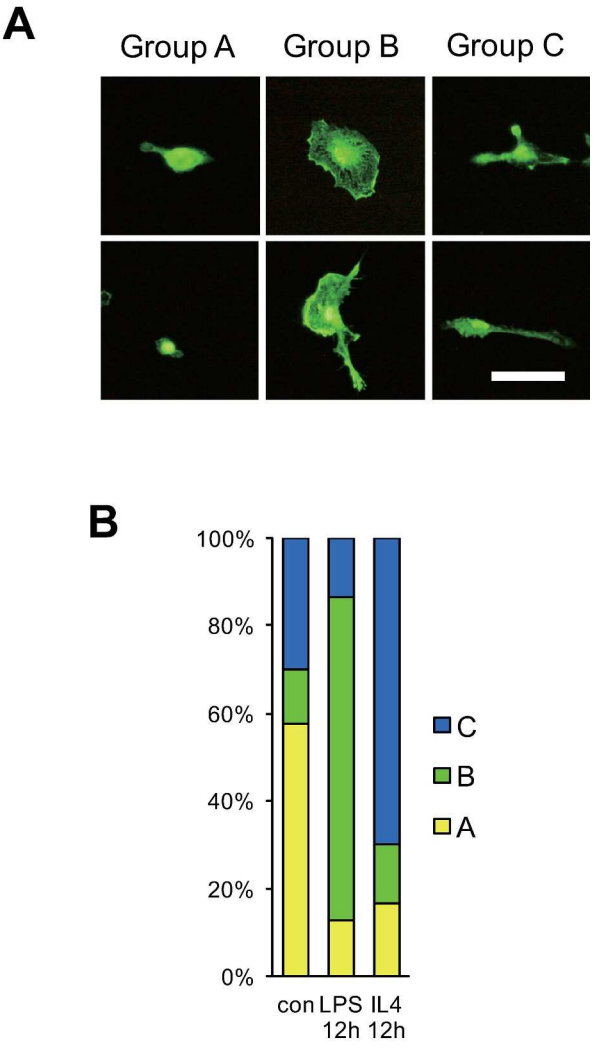

226x418mm (300 x 300 DPI)

Supplementary Fig. 4

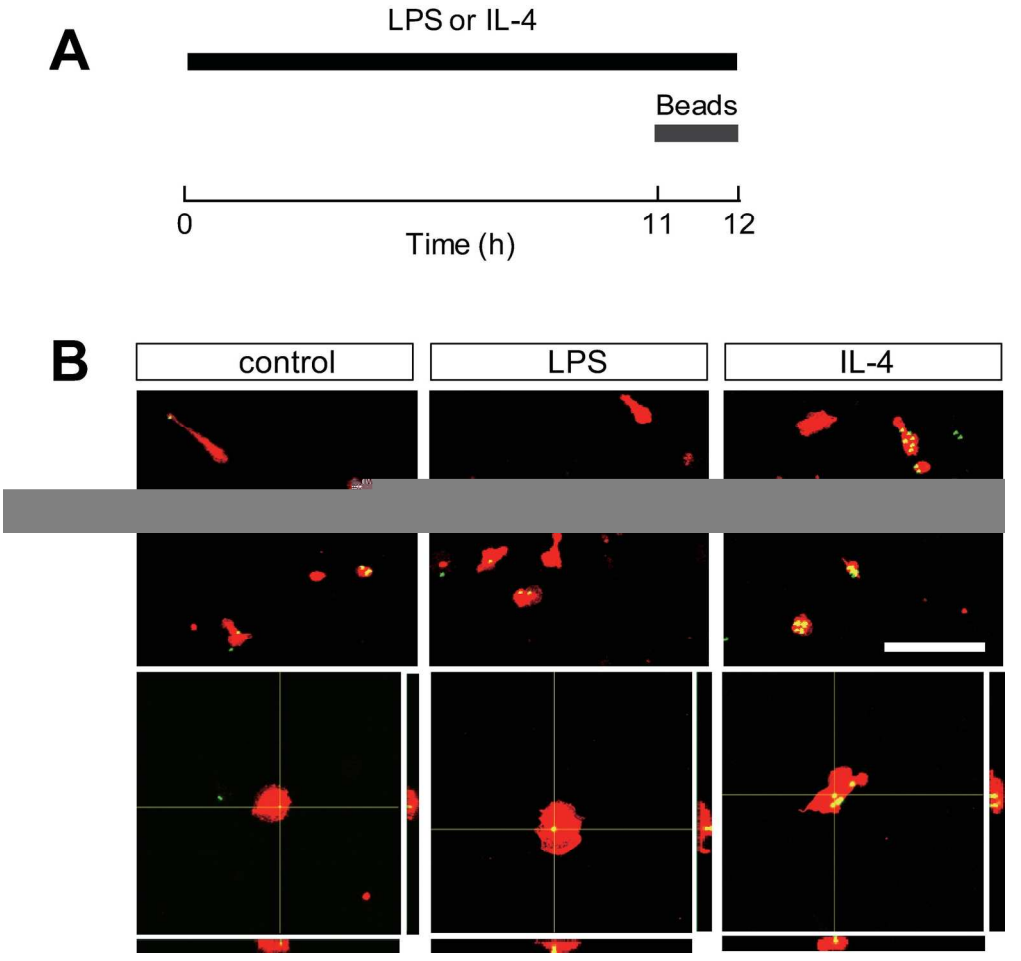

173x200mm (300 x 300 DPI)

Supplementary Fig. 5

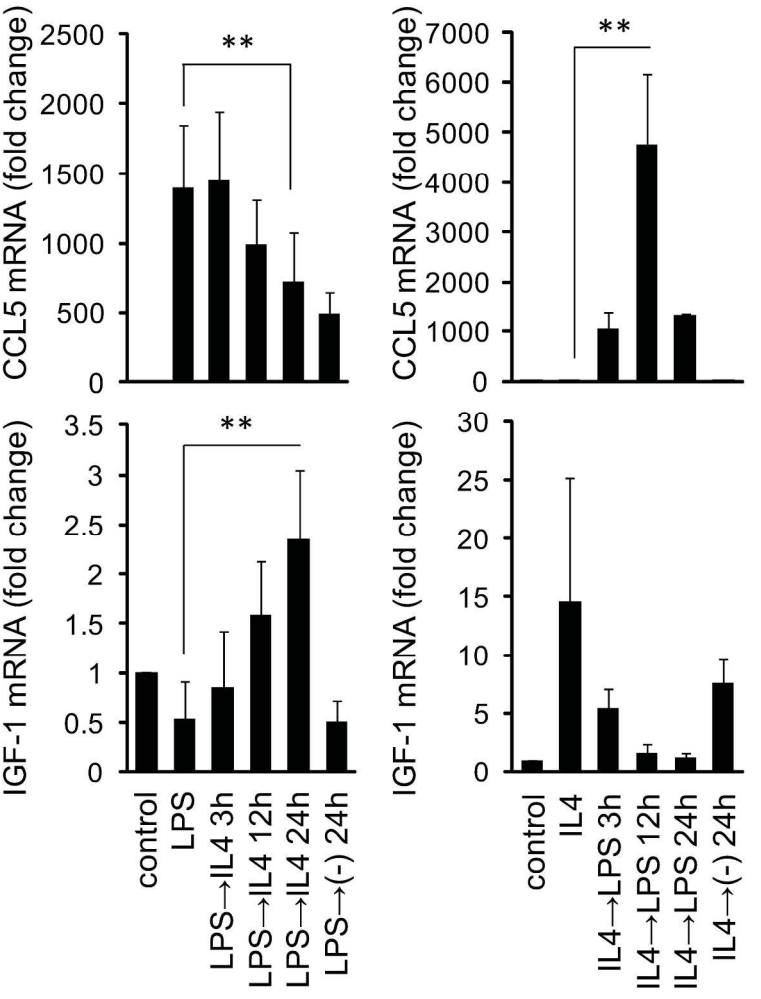

227x309mm (300 x 300 DPI)

Supplementary Fig. 6

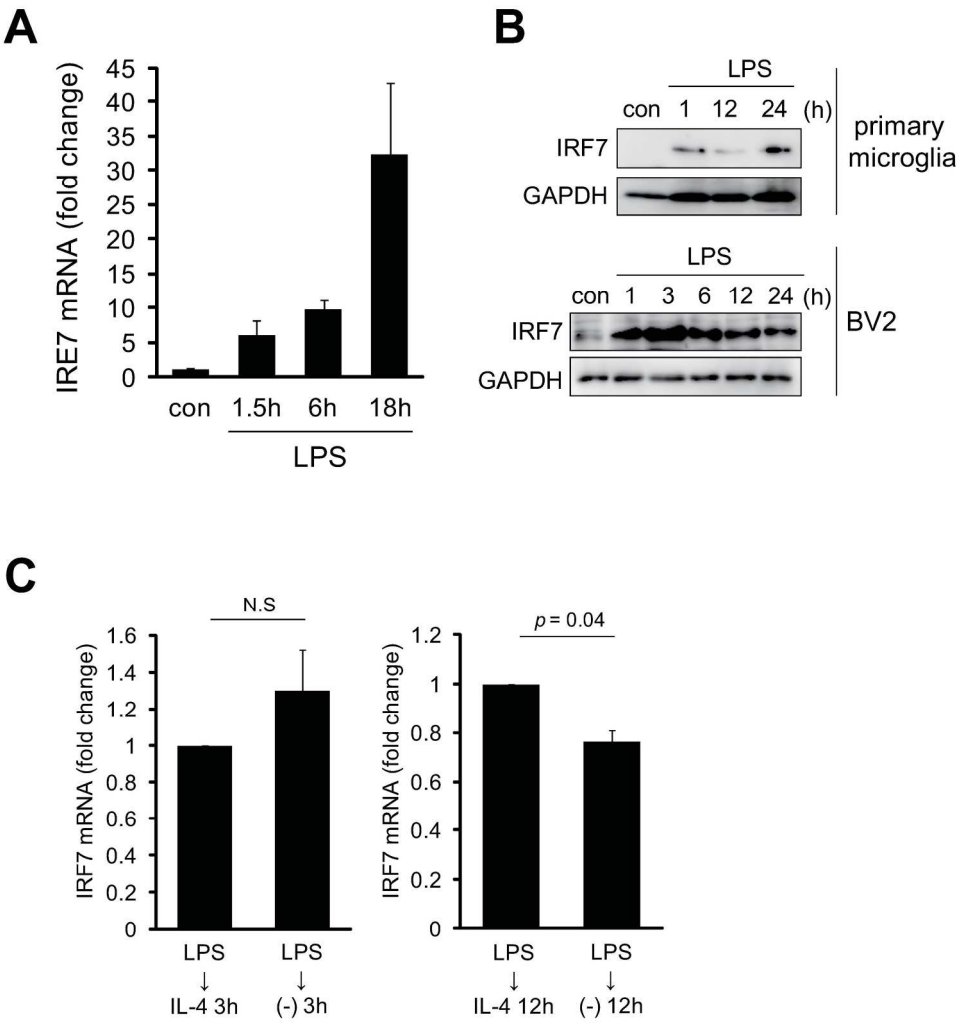

208x241mm (300 x 300 DPI)

Supplementary Fig. 7

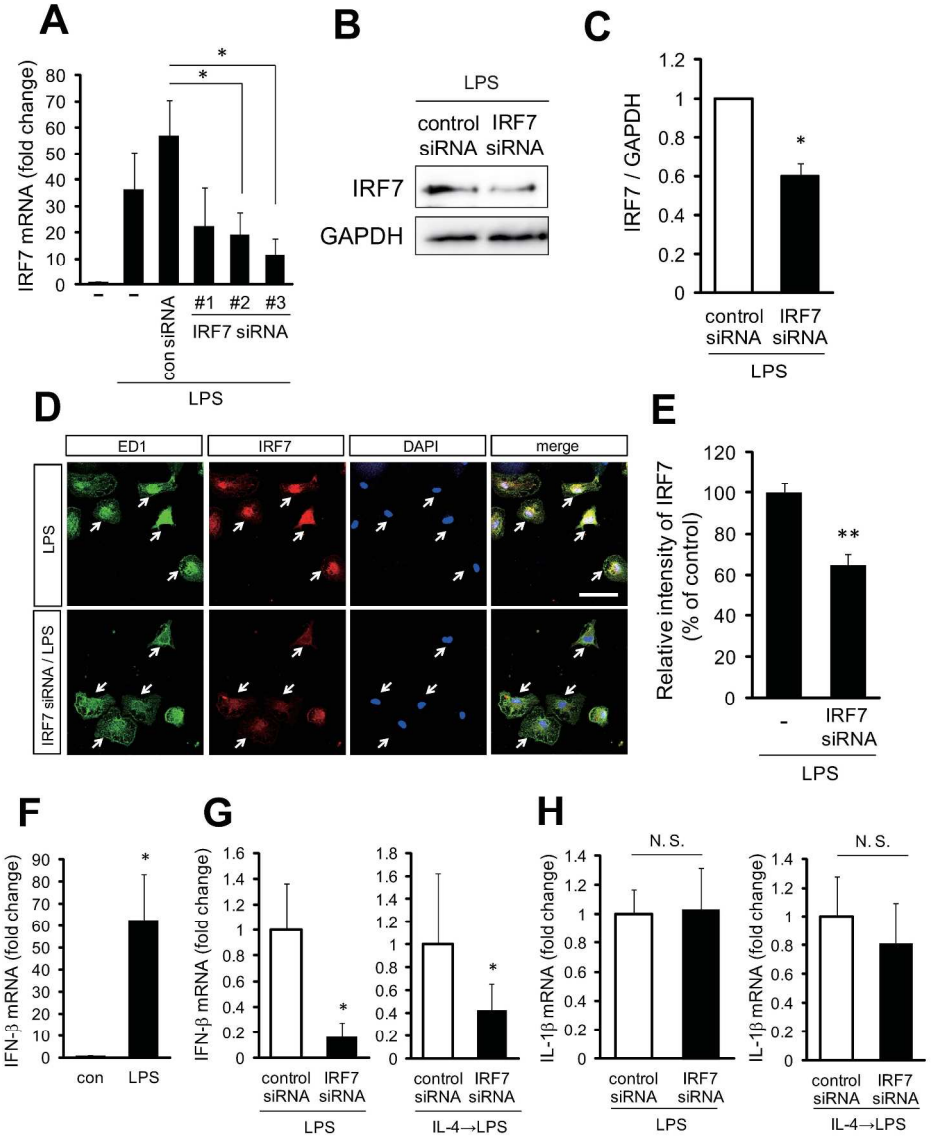

249x319mm (300 x 300 DPI)

Figure of Main Points

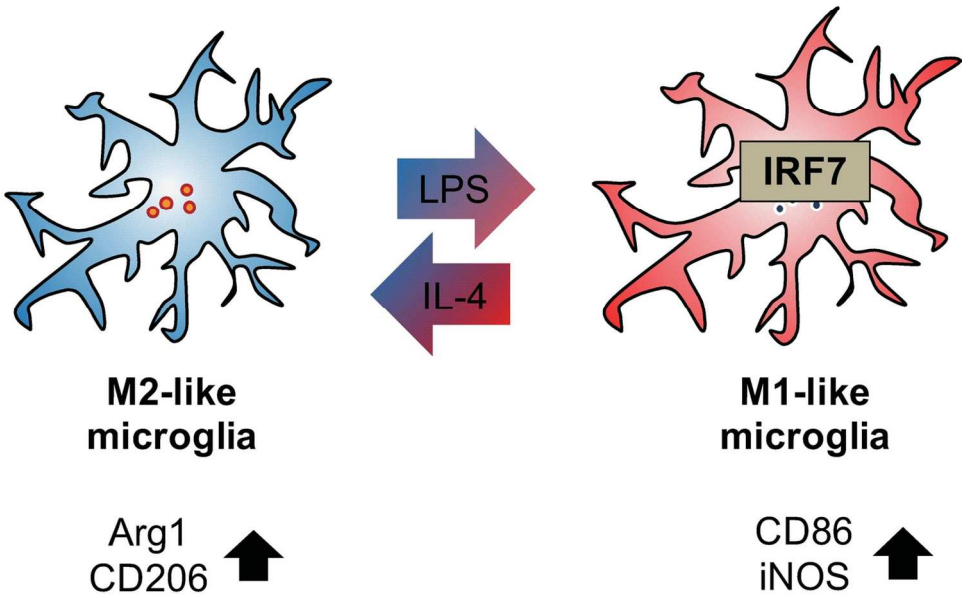

Microglial phenotypes are regulated by extracellular stimulus.
Interferon regulatory factor 7 is elevated in M1-like microglia and is associated with microglial polarization.

132x118mm (300 x 300 DPI)